A Stochastic Controller for Primary Frequency Regulation Using ON/OFF Demand Side Resources

Guanyu Tian and Qun Zhou Sun, *Member, IEEE*

***Abstract*—Residential ON/OFF devices, such as thermal-controlled loads and smart appliances, have great potential for providing frequency regulation service in the power grid. These devices can be engaged using centralized, distributed, or local control. However, both centralized and distributed controls require significant costs for communication infrastructure, while local controllers may perform poorly due to a lack of coordination. To address the challenges, a stochastic demand-side management controller is proposed. The stochastic controller dynamically adjusts the aggregated response power profile by randomizing the execution of demand response actions using a stochastic filter with no communication required. The system frequency response is analytically proved to be critically damped to the nominal value. Using the stochastic controller on grid-interactive water heaters, test cases are implemented to validate the frequency regulation performance under a power system transient scenario. The proposed controller produces the best system frequency response compared to benchmark controllers.**

***Index Terms*—Demand response, frequency regulation, stochastic controller, water heaters.**

I. Introduction

THERMAL controlled loads and smart appliances, such as water heaters (WH) and air conditioners (AC), are the flexible loads in residential houses that are playing increasingly important roles in providing grid services, especially the primary frequency regulation [1], [2]. These demand-side resources are mainly ON/OFF devices. In the existing literature, ON/OFF devices can be used for frequency regulation in three ways, centralized, distributed, or locally controlled [3], [4], [5].

Centralized and distributed controls require communication to a control center or neighboring controllers, which tremendously increases the cost of implementation and potentially introduces vulnerability from cyber-attacks. In contrast, local controllers avoid the need for communication infrastructure by responding to local frequency information. The response logic of a locally controlled ON/OFF device is to mitigate the power imbalance by turning off the controlled device when the monitored local frequency is lower than the nominal frequency and vice versa. To avoid frequent switching, the time-variant frequency dead band scheme has been proposed in [6].

Manuscript received 9 December 2022; revised 8 April 2023; accepted 5 May 2023. Date of publication 30 June 2023; date of current version 23 August 2023. This work was supported by the U.S. Department of Energy's Office of Energy Efficiency and Renewable Energy (EERE) under the Building Technology Office, BENEFIT 2019 under Award DE-EE0009152. Paper no. PESL-00324-2022. *(Corresponding author: Guanyu Tian.)*

The authors are with the Department of Electrical and Computer Engineering, University of Central Florida, Orlando, FL 32816 USA (e-mail: tiang@knights.ucf.edu; QZ.Sun@ucf.edu).

Color versions of one or more figures in this article are available at https://doi.org/10.1109/TSG.2023.3291218.

Digital Object Identifier 10.1109/TSG.2023.3291218

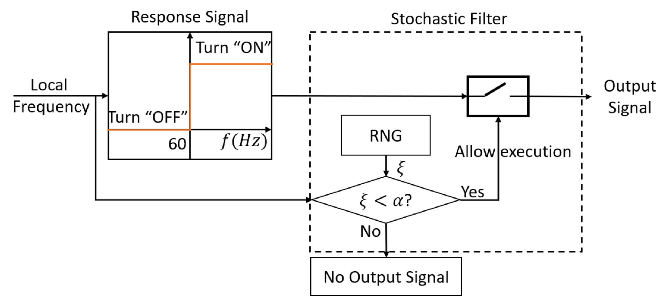

Fig. 1. Design of the S-DSM controller for ON/OFF devices.

However, the existing local controller has significant drawbacks that prevent it from being widely adopted despite its low cost. First, as the system frequency rarely falls exactly on the nominal value, frequent ON/OFF switching of devices may occur and reduce the life cycle. Frequency dead bands can be used, but the frequency response would most likely either converge to a non-nominal value or oscillate within the band [6]. In addition, all devices using the local control scheme respond to the same signal simultaneously, resulting in a systematic shock and frequency oscillation to the grid. This effect is further demonstrated in our case study.

This letter proposes a novel stochastic demand-side management (S-DSM) controller for ON/OFF devices to provide frequency regulation. The proposed stochastic controller is a local controller that does not require communication infrastructure. It operates without any dead band while achieving good performance in conjunction with internal controls. The convergence of frequency response is analytically proved to be critically damped to the nominal value without oscillation.

II. Methodology

A. Stochastic Demand Response Controller

Fig. 1 illustrates the control logic of the proposed S-DSM controller. The principle is to randomize the response status among ON/OFF devices. The S-DSM controller is composed of a logic controller and a stochastic filter. It generates control signals based on the comparison between the measured frequency f and nominal frequency f_0: $f < f_0$ produces an "OFF" signal and $f > f_0$ produces an "ON" signal. The stochastic filter is triggered every Δt second and samples a uniform random number ξ in the range of [0, 1]. The control signal is executed only when $\xi < \alpha$; otherwise, it is bypassed.

Note that the S-DSM controller works seamlessly with the device's internal controls, e.g., the internal controller of a water heater with temperature bounds. The frequency control signal will be executed when the temperature is within the bounds; otherwise, the internal controller will overwrite it to ensure the intended water heating functionality. Although alternative overwriting can happen, its probability, denoted by α^N, decreases exponentially with the number of overwriting N. Hence, frequent overwriting/switching rarely happens in practice. This feature is further demonstrated in the case study.

In addition, the S-DSM controller eliminates the need for frequency dead bands while improving the system frequency convergence. Thanks to its stochastic nature, the S-DSM controller guarantees the convergence of frequency to the nominal value exactly, in contrast to deterministic dead band-based controllers that yield constant frequency errors. The frequency convergence is analytically proved in the next section. During normal frequency fluctuations, consecutive switching can happen, but its probability, denoted by α^M, decreases exponentially with the number of fluctuations M.

Given a large number of ON/OFF devices, this control scheme effectively turns on an α portion of devices that are currently in OFF mode when the frequency is higher than the nominal value; and turns off an α portion of devices that are currently in ON mode when the frequency is lower than the nominal value. The aggregated performance of a large number of S-DSM-controlled devices is summarized in Algorithm 1, where f_t and r_t denote the system frequency and the ratio of devices in ON mode at the time step t.

Algorithm 1: S-DSM Controller Aggregated Performance

```
for Every Δt seconds do
    Input: f_t, r_t
    Output: r_{t+1}
    if f_t < f_0 then
        Under-frequency mode triggered:
            • Reduce load by turning off an α portion of
              water heaters in ON mode.
            • Update: r_{t+1} = (1 − α)r_t
    end
    if f_t > f_0 then
        Over-frequency mode triggered:
            • Increase load by turning on an α portion of
              water heaters in OFF mode.
            • Update: r_{t+1} = r_t + (1 − r_t)α
    end
    if f_t = f_0 then
        Neither mode is triggered:
            • Maintain current operation status.
            • Update: r_{t+1} = r_t
    end
end
```

B. Proof of Convergence

To show that the system frequency converges to the nominal value under the proposed S-DSM controller, it is necessary to construct the dynamic model and show that the frequency response is stable. The state variables of interest in the dynamic system of frequency regulation are ω, the machine speed, and r, the ratio of ON/OFF devices in ON mode. The dynamic model of ω is formulated in (1), where P_m and P_e denote the mechanical power and electrical power output of the generator, H is the time constant related to the inertia and D is the damping coefficient of the generator. ω_0 denotes the nominal machine speed [7].

$$\dot{\omega} = \frac{1}{2H}(P_m - P_e - D(\omega - \omega_0)) \tag{1}$$

Assuming line losses are neglected, the real power balance at the generator bus is (2), where the electrical power output P_e equals the summation of the non-responsive load P_d and the responsive load P_r. P_r^{Total} denotes the capacity of all ON/OFF devices in the system.

$$P_e = P_d + rP_r^{Total} \tag{2}$$

Depending on the response mode, under-frequency or over-frequency, the dynamic models for r are different.

1) Under-Frequency Mode: In the under-frequency mode, the discrete form of r transition is (3). The slope of r can be approximated by $\frac{r_{t+1}-r_t}{\Delta t}$ in (4). Taking the slope as the derivative, the dynamic model of r can be obtained in (5).

$$r_{t+1} = r_t(1-\alpha) \tag{3}$$
$$\frac{r_{t+1} - r_t}{\Delta t} = -\frac{\alpha r_t}{\Delta t} \tag{4}$$
$$\dot{r} = -\frac{\alpha r}{\Delta t} \tag{5}$$

2) Over-Frequency Mode: In the over-frequency mode, the discrete form of r transition is (6). The slope of r can be approximated by $\frac{r_{t+1}-r_t}{\Delta t}$ in (7). Taking the slope as the derivative, the dynamic model of r can be obtained in (8).

$$r_{t+1} = r_t + (1-r_t)\alpha \tag{6}$$
$$\frac{r_{t+1} - r_t}{\Delta t} = \frac{(1-r_t)\alpha}{\Delta t} \tag{7}$$
$$\dot{r} = \frac{(1-r)\alpha}{\Delta t} \tag{8}$$

Let $x = [\omega \quad r]^T$ be the state vector, the matrix form of the system dynamic model in under-frequency mode and over-frequency mode can be obtained in (9) and (10) respectively.

$$\dot{x} = \begin{bmatrix} -\frac{D}{2H} & -\frac{P_r^{Total}}{2H} \\ 0 & -\frac{\alpha}{\Delta t} \end{bmatrix} x + \begin{bmatrix} \frac{P_m - P_d + D\omega_0}{2H} \\ 0 \end{bmatrix} \tag{9}$$
$$\dot{x} = \begin{bmatrix} -\frac{D}{2H} & -\frac{P_r^{Total}}{2H} \\ 0 & -\frac{\alpha}{\Delta t} \end{bmatrix} x + \begin{bmatrix} \frac{P_m - P_d + D\omega_0}{2H} \\ \frac{\alpha}{\Delta t} \end{bmatrix} \tag{10}$$

It can be observed that the transition matrix is the same for both modes, and the eigenvalues are $\lambda_1 = -\frac{\alpha}{\Delta t}$ and $\lambda_2 = -\frac{D}{2H}$. Considering $\alpha, \Delta t, D,$ and H are all positive real numbers, both eigenvalues are negative real numbers. Hence, the system must be stable and critically damped, proving the convergence of Algorithm 1.

C. Steady-State Frequency

In this section, we will prove that the system frequency is converging to either a small bound near the nominal value or strictly at the nominal value in the steady state under two settings of the probability threshold, i.e., constant α and dynamic α. We recommend the dynamic α in real-world implementations for its superior converging performance.

1) Constant α: The steady-state is obtained where $\dot{x} = \mathbf{0}$. For machine speed, the steady-state solution ω_{ss} can be obtained in (11) from (1), where r_{ss}, the steady state solution

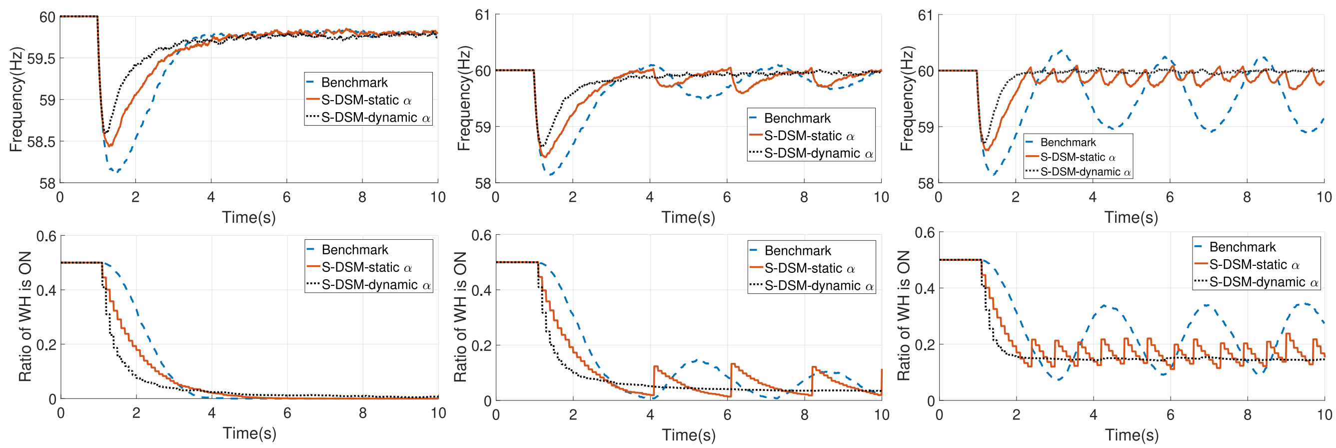

(a) #GIWH=1800 (b) #GIWH=2100 (c) #GIWH=2800

Fig. 2. Performance comparison.

TABLE I
SIMULATION PARAMETERS

Parameter	Value	Parameter	Value
α	0.1	k	10
ω_0	1 p.u.	f_0	60 Hz
H	20 s	D	3 p.u.
P_m	10 p.u.	Δt	0.1 s
P_{WH}	1e-4 p.u.		

of the ratio of devices in ON mode, determines the frequency deviation in steady state.

$$\omega_{ss} = \omega_0 + \frac{P_m - P_d - r_{ss}P_r^{Total}}{D} \tag{11}$$

In under-frequency response mode (5), $r_{ss} = 0$; in over-frequency response mode (8), $r_{ss} = 1$. Consequently, the frequency deviation is bounded by $[2\pi \frac{P_m - P_d - P_r^{Total}}{D}, 2\pi \frac{P_m - P_d}{D}]$.

2) Dynamic α: To eliminate the steady-state frequency deviation caused by constant α, ω is expected to converge to the nominal value ω_0, while r converges to its steady-state solution as well. Thus, a dynamic α that satisfies the criterion in (12) is needed.

$$\lim_{\omega \to \omega_0} \dot{r} = 0 \tag{12}$$

Considering α is the coefficient in (5) and (8), the criterion (12) is satisfied for both modes as long as (13) holds.

$$\lim_{\omega \to \omega_0} \alpha = 0 \tag{13}$$

Here we select the absolute error function in (14) to formulate the dynamic α, where k is a constant coefficient that adjusts the scale. Note that the formulation of dynamic α is not unique.

$$\alpha = k|\omega - \omega_0| \tag{14}$$

III. CASE STUDY

To validate the performance of the proposed S-DSM controller, a case study of frequency regulation using grid-integrated water heater (GIWH) units is performed. The parameters used in the transient simulation are summarized in Table I. P_{WH} denotes the average power of a GIWH unit. The simulation resolution is 0.01 seconds and is performed in MATLAB on a desktop computer with a 4-core 3.2 GHz CPU and 16 GB RAM.

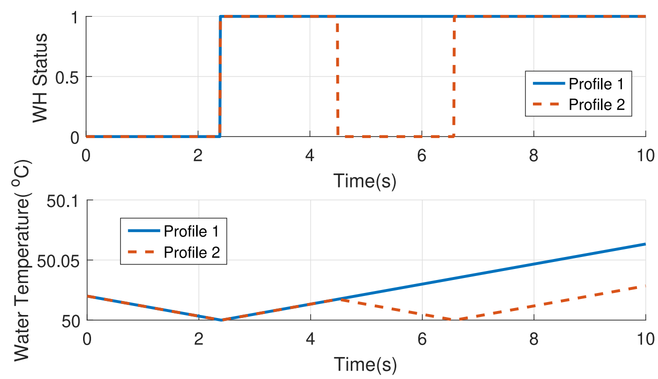

Fig. 3. Typical switching and temperature profiles under scenario (c) with dynamic α.

Three test scenarios with 1800, 2100, and 2800 GIWH units are considered. Half of the GIWHs are initially ON, and their water temperatures are randomly selected within the normal operating range, i.e., 50°C ∼ 60°C. The linear approximation temperature dynamic model from [8] is used. At time 1s, a transient occurs when the non-responsive load P_d increases by 0.1 p.u.

Fig. 2 shows the performance of benchmark, constant α, and dynamic α controllers under the three scenarios. The benchmark method is a local controller with time-varying dead bands and randomized response time [6]. All three controllers achieve the same steady-state frequency at different convergence rates under the lowest GIWH penetration level (insufficient to restore frequency to 60 Hz). At higher penetration levels, the benchmark and static α controllers experience oscillations, while the dynamic α controller maintains critical damping convergence to 60 Hz.

Fig. 3 shows two typical ON/OFF switching and temperature profiles under scenario (c) with dynamic α. Temperature is well maintained while the system frequency is converging. Profile 2 represents devices that are switched 3 times, but this

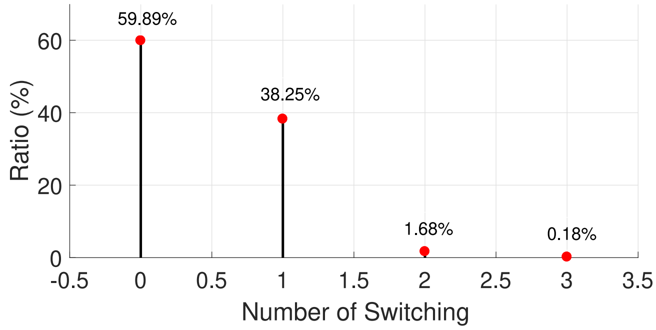

Fig. 4. Distribution of the number of switching.

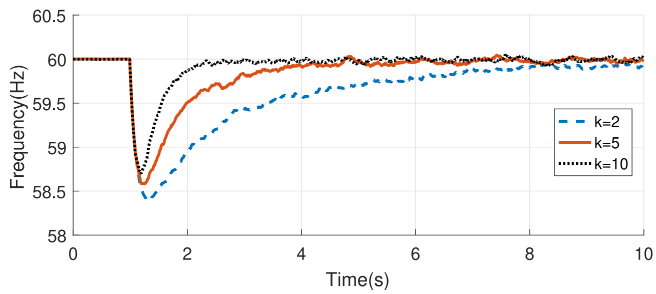

Fig. 5. A sensitivity study on k.

is only a small portion. Indeed, Fig. 4 shows the probability distribution of the number of switching, where only 0.18% devices are switched three times within 10 seconds, indicating that frequent switching rarely occurs.

Parameter sensitivity is also studied, specifically, the coefficient k that determines the probability of being selected in dynamic α. Fig. 5 suggests that a larger k leads to a faster convergence rate. Note that increasing k also increases the chance of over-response, and hence a careful design of k needs further investigation in our future work.

IV. Conclusion

In this letter, a novel stochastic controller is proposed for primary frequency regulation using ON/OFF devices. The convergence of the S-DSM controller performance is proved, and the steady-state frequency reaches the nominal value with a dynamic probability threshold. The proposed controller is a local controller that requires no communication infrastructure. In addition, it can be easily plugged into existing devices and work seamlessly with the internal controls. Simulation results validate the frequency convergence using grid-integrated water heater units while maintaining their functionality without frequent switching. In future work, more efforts will be focused on control parameter design. This work will also be expanded to cover new types of devices.

References

[1] B. Biegel, L. H. Hansen, P. Andersen, and J. Stoustrup, "Primary control by ON/OFF demand-side devices," *IEEE Trans. Smart Grid*, vol. 4, no. 4, pp. 2061–2071, Dec. 2013.

[2] M. Song, G. Ciwei, J. Yang, Y. Liu, and G. Cui, "Novel aggregate control model of air conditioning loads for fast regulation service," *IET Gener. Transm. Distrib.*, vol. 11, no. 17, pp. 4391–4401, 2017.

[3] T. Masuta and A. Yokoyama, "Supplementary load frequency control by use of a number of both electric vehicles and heat pump water heaters," *IEEE Trans. Smart Grid*, vol. 3, no. 3, pp. 1253–1262, Sep. 2012.

[4] X. Kou et al., "A comprehensive scheduling framework using SP-ADMM for residential demand response with weather and consumer uncertainties," *IEEE Trans. Power Syst.*, vol. 36, no. 4, pp. 3004–3016, Jul. 2021.

[5] K. Samarakoon, J. Ekanayake, and N. Jenkins, "Investigation of domestic load control to provide primary frequency response using smart meters," *IEEE Trans. Smart Grid*, vol. 3, no. 1, pp. 282–292, Mar. 2012.

[6] A. Molina-Garcia, F. Bouffard, and D. S. Kirschen, "Decentralized demand-side contribution to primary frequency control," *IEEE Trans. Power Syst.*, vol. 26, no. 1, pp. 411–419, Feb. 2011.

[7] G. Tian, Q. Zhou, R. Birari, J. Qi, and Z. Qu, "A hybrid-learning algorithm for Online dynamic state estimation in multimachine power systems," *IEEE Trans. Neural Netw. Learn. Syst.*, vol. 31, no. 12, pp. 5497–5508, Dec. 2020.

[8] S. Xue, Y. Che, W. He, Y. Zhao, and R. Zhang, "Control strategy of electric heating loads for reducing power shortage in power grid," *Processes*, vol. 7, no. 5, p. 273, 2019.